# Study of the Conformation of Bromated Guanidines with Potential Anti-Leishmania Activity

Eduardo Henrique Zampieri , Luana Ribeiro Dos Anjos , Pedro Henrique de Oliveira Santiago , Tainara Rosário da Silva Nascimento , Javier Alcides Ellena , Eduardo René Pérez González *

Posted Date: 22 December 2023

doi: 10.20944/preprints202312.1728.v1

Keywords: Guanidines compounds; Leishmaniasis; Bromination; NBS; X-ray and NMR conformational study

*Article*

# Study of the Conformation of Bromated Guanidines with Potential Anti-Leishmania Activity

**Eduardo Henrique Zampieri [1], Luana Ribeiro dos Anjos [1], Pedro Henrique de Oliveira Santiago [2], Tainara Rosário da Silva Nascimento [1], Javier Alcides Ellena [2] and Eduardo René Pérez González [1, *]**

[1] Fine Organic Chemistry Lab, School of Sciences and Technology, São Paulo State University (UNESP), Presidente Prudente 19060-080, Brazil; eduardo.h.zampieri@unesp.br, luana.anjos@unesp.br, tainara.nascimento@unesp.br
[2] Multiuser Structural Crystallography Laboratory, São Carlos Institute of Physics, University of São Paulo (USP), São Carlos 13566-590, Brazil; pedrophs.santiago@gmail.com, javiere@if.sc.usp.br
* Correspondence: eduardo.gonzalez@unesp.br

**Abstract:** Leishmaniasis are neglected diseases that affect regions such as South Asia, South Africa and Latin America, less developed regions. Current treatment, for cutaneous, mucocutaneous and visceral leishmaniosis, which are the main forms of the disease, is based on the administration of pentavalent antimonial and amphotericin B. However, these drugs have low efficacy and high toxicity. For this reason, the search for new treatments for this disease is necessary, based on studies of new molecules and their conformations. The research proposed the conformational study of brominated guanidine compounds with potential antileishmanial activity using Nuclear Magnetic Resonance (NMR) and X-ray diffraction (XRD) techniques. The study involved two brominated molecules, LQOF-G35 and LQOF-G35-Br. The later was synthesized by the reaction of LQOF-G35 and NBS under IR irradiation at 120 Watts of potency and dichloromethane as solvent by 12-h of exposition. The obtained results demonstrated the efficiency of the bromination method, since two bromines atoms entered the molecule. Furthermore, NMR analysis show the occurrence of a *Z* to *E* conformational change. This feature was well confirmed by comparative DRX study of the LQOF-G35 and LQOF-G35-Br compounds.

**Keywords:** Guanidines compounds; Leishmaniasis; Bromination; NBS; X-ray and NMR conformational study

## 1. Introduction

The research and development of drugs to treat diseases, such as leishmaniasis, involves the creation of molecules through pharmacological design, synthesis, and biological and structural characterization. Leishmaniasis, prevalent in Southeast Asia, Sub-Saharan Africa and Latin America [1], encompasses several clinical-pathological manifestations, among them the most common known as cutaneous leishmaniasis, caused by Leishmania amazonensis, manifests itself through lesions and ulcers on the skin, and the most severe, visceral leishmaniasis, is characterized by anemia, significant weight loss, enlarged spleen, fever and often results in death, the latter being observed in 85-90% of untreated cases [1,2,3].

Current treatments, such as chemotherapy with pentavalent antimonials, paromomycin, amphotericin B, and miltefosine, present challenges, including low efficacy and severe side effects such as cardiotoxicity, pancreatitis, hepatotoxicity, parasite resistance, and long-term administration [2-5]. Therefore, the search for safer and more effective antileishmania compounds against leishmaniasis is essential [4,5,6].

Guanidine compounds are often found in nature and used in the synthesis of a variety of organic compounds, such as quinazolines, oxazolidinones, lactones, and carbonates [7-11]. Novel guanidine derivatives exhibit several biological effects, such as cardiovascular dilation, antihistamine properties, anti-inflammatory activity, antidiabetic effects, antibacterial, antifungal, antiprotozoal/antiparasitic properties, and antiviral activity [7,12-21]. Recently, some guanidine compounds have been studied in relation to leishmaniasis [22,23].

 doi:10.20944/preprints202312.1728.v1



In 2019, Espírito Santo R. D. *et al.*, carried out the structural characterization by nuclear magnetic resonance (NMR) and the evaluation of the antiparasitic activity of a series of guanidine compounds [20], in this study some compounds proved to be highly effective and promising due to their low toxicity against mammals and high lethality for parasites. One such compound was LQOF-G2, which has the bromo atom in the "*para*" position of the aniline ring.

This compound stood out as the most effective candidate against leishmaniasis in the study, with a preferential 'Z' conformation being observed [22]. Another guanidine compound, LQOF-G35, which has a bromine atom as a substituent in the "*ortho*" position of the aniline ring, was studied in relation to Leishmania amazonensis and Leishmania braziliensis in the promastigote forms. This compound demonstrated an $IC_{50}$ value of 29.82 and 25.87 μM, respectively, standing out as an even more promising candidate when looking at the $IC_{50}$ values in amastigotes 7.63 and 4.62, respectively [24].

Based on these reported results, it was decided to examine the effects of incorporating additional bromine atoms into the structure of the guanidine compound LQOF-G35. Therefore, the bromination reaction with *N*-Bromosuccinimide was performed using irradiation with an IR lamp [25-30] and the results are described here.

## 2. Results and Discussion

The characterization of the compounds was carried out initially by electronic ionization mass spectrometry and melting point measurements (Table 1).

**Table 1.** Melting point and molecular ion data for guanidines.

| Compound | Melting point (°C) | Molecular Ion [M]+ |
|---|---|---|
| LQOF-G35 | 103.0 – 104.0 | 406 *m/z* |
| LQOF-G35-Br | 147.9 – 149.6 | 565 *m/z* |

LQOF-G35-Br also was studied by high resolution mass spectrometry with electrospray ionization in the positive ion mode (ESI(+)-MS) and was identified by the detection of their intact protonated molecule, which were selected and further fragmented via ESI(+)-MS/MS experiments. Figure S3 shows the HRESI(+)-MS and ESI(+)-MS/MS spectra of the compound LQOF-G35-Br (m/z 565.8898 [M+H]+). The ESI(+)-MS/MS experiments yielded fragment ions at m/z 487 and 365 that are in agreement with formation of the desired product.

NMR studies were conducted at -10°C (263K) for LQOF-G35 and 10°C (283K) for LQOF-G35-Br. The NMR spectra can be found in the supplementary material and the most relevant data are highlighted in the Table 2.

The $^{1}H$ NMR of LQOF-G35 revealed the signals of the hydrogens NH 1 and 2, with chemical shifts of 5.19 and 12.33 ppm respectively, which were confirmed by HMBC $^{1}Hx^{15}N$ (Figure S4). In contrast, the NH 1 and 2 hydrogens of LQOF-G35-Br were observed at 8.56 and 8.30 ppm respectively. This difference is due to the stabilization of both different conformations by the formation of a hydrogen bond between the hydrogen atom of the coplanar NH groups and the carbonyl oxygen atom, forming a pseudo six-member cycle. In this way, the NH hydrogen atom involves in the intramolecular hydrogen bond becomes less shielded. Therefore, it is possible to state that there was a conformational change from *Z* to *E* after or simultaneously bromination. This result was confirmed by XRD study (Figure 2).

Another important signal for LQOF-G35-Br was observed at 7.73 ppm, a singlet that integrates two protons, this signal represents the hydrogens H5/H7 (chemically equivalent). Which was also confirmed by HMBC $^{1}Hx^{13}C$ due to its correlations with four $^{13}C$ signals, three of which are associated with quaternary carbons (C4/C8 115.4 ppm, C3 119.3 ppm and C6 143.6 ppm), as well as the linker carbon C5/C7 itself, observed at 134.6 ppm.

**Table 2.** Chemical shifts (ppm) obtained by $^{13}C$ NMR (500 MHz; $CDCl_3$) of guanidine compounds.

Preprints (www.preprints.org) | NOT PEER-REVIEWED | Posted: 22 December 2023 doi:10.20944/preprints202312.1728.v1



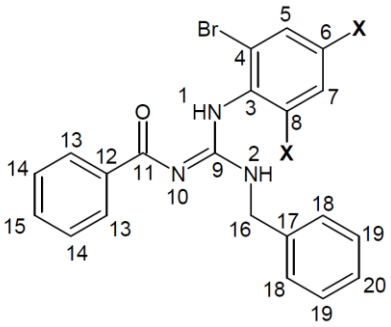

**LQOF-G35.** X = H
**LQOF-G35-Br.** X = Br

| | HYDROGENS | | | | | | | | | |
|---|---|---|---|---|---|---|---|---|---|---|
| | **H1** | **H2** | **H5** | **H8** | **H10** | **H13** | **H14** | **H16** | **H18** | **H19** |
| **LQOF-G35** | 5.19 | 12.33 | 7.68 | 7.31 | - | 8.30 | 7.43 | 4.76 | 7.38 | 7.38 |
| **LQOF-G35-Br** | 8.56 | 8.30 | 7.73 | - | 7.56 | 7.56 | 7.49 | 4.72 | 7.48 | 7.37 |

| | CARBONS | | | | | | | | | | | |
|---|---|---|---|---|---|---|---|---|---|---|---|---|
| | **C3** | **C4** | **C6** | **C8** | **C9** | **C11** | **C12** | **C13** | **C14** | **C16** | **C17** | **C18** |
| **LQOF-G35** | 138.1 | 121.5 | - | - | 158.1 | 177.7 | 138.4 | 129.3 | 128.1 | 45.0 | 134.8 | 127.8 |
| **LQOF-G35-Br** | 119.3 | 115.4 | 143.6 | 115.4 | 144.4 | 166.7 | 132.8 | 127.1 | 127.7 | 45.1 | 138.1 | 129.2 |

Aliphatic hydrogens (H16) were identified at 4.7 ppm, corroborated by the HSQC $^{1}Hx^{13}C$ technique. Aromatic hydrogens were observed in the region between 7.0-8.5 ppm.

Through $^{13}C$ NMR it was possible to observe the C16 aliphatic signal for both guanidines. Between 115 and 166 ppm, all remaining carbons in the structures were observed. However, for LQOF-G35-Br there was the appearance of an additional quaternary carbon compared to LQOF-G35. Initially, this signal could indicate mono bromination in the structure. However, one of the bromines bonds (in ortho) makes carbons C4 and C8 chemically equivalent, resulting in only one signal for these and another for C6 (para position).

In conjunction with these analyses, a NOESY study was conducted, providing corroborating spatial information between hydrogens. Figure 1 illustrates the main spatial correlations for guanidines. We can observe intense correlations between H2-H16 and H18-H16 for LQOF-G35, with emphasis on the H13-H16 and H8-H2 correlations, what indicate the *Z* conformation. For LQOF-G35-Br, intense correlations were observed between H1-H16, H18-H16 and H19-H16, therefore, indicating the *E* conformation.

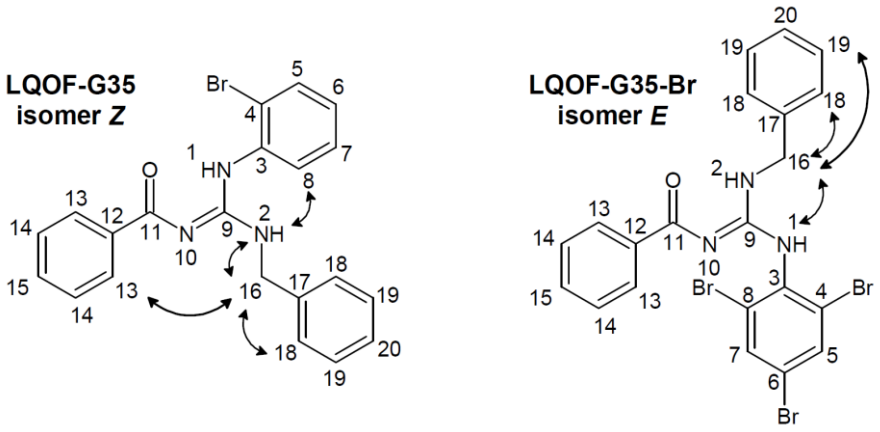


**Figure 1.** Conformational NOESY of guanidines LQOF-G35 and LQOF-G35-Br.

Single crystals of both compounds were obtained and analyzed using the SCXRD tech-nique. The compound LQOF-G35 crystallizes in the non-centrosymmetric trigonal space group $P3_2$ and contains three independent molecules in the asymmetric unit, as shown in Figure 2. The SCRXD

Preprints (www.preprints.org) | NOT PEER-REVIEWED | Posted: 22 December 2023 doi:10.20944/preprints202312.1728.v1



study of LQOF-G35 show that the guanidine group present a resonant structure, with C–N bond distances ranging from 1.330 Å to 1.357 Å, formed by the contribution of the different resonance hybrids. As indicated by the NMR analyses, the LQOF-G35 has the *Z* conformation, with the amine group from the aniline stabilized by a six membered ring intramolecular hydrogen bond, N1H···O1. The presence of the hydrogen atoms bonded to the nitrogen atoms from the aniline and aminobenzyl groups was also indicated by the SCXRD analysis, with the evaluation of the electronic density maps.

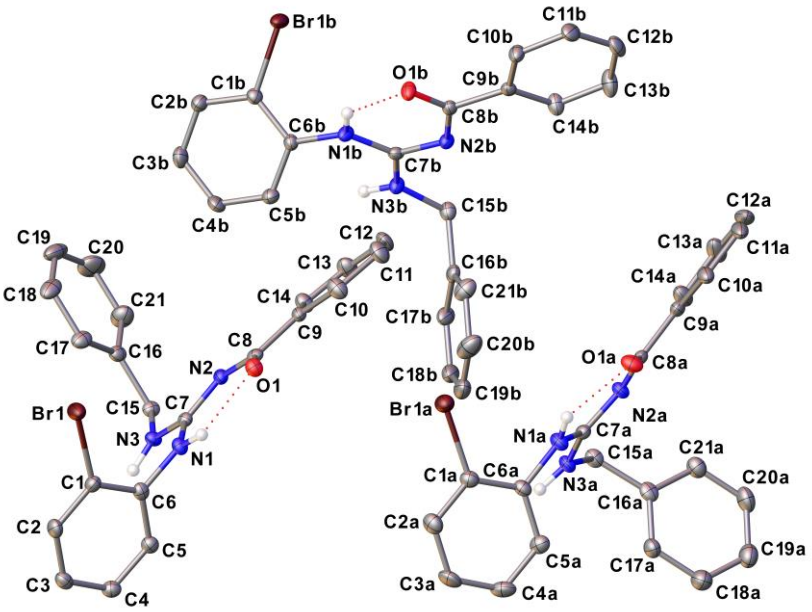


**Figure 2.** ORTEP type representation of the asymmetric unit of LQOF-G35, with thermal ellipsoids represented with 50% of probability. Hydrogen atoms bonded to the carbon atoms were omitted for clarity.

On the other hand, compound LQOF-G35-Br crystallized in the monoclinic space group $P2_{1/c}$, containing just one molecule per asymmetric unit (Figure 3). The analysis of the C-N bond lengths of the guanidine group, C7–N1 (1.290(3) Å), C7–N2 (1.409(3) Å) and C7–N3 (1.348(3) Å), indicate that the double bond is not in resonance in this case, just involving the atoms C7 and N1. An inversion in the position of the aniline and aminobenzyl groups was verified in the structure of LQOF-G35-Br, presenting an *E* conformation about the C7–N2, being now stabilized by another six membered ring intramolecular hydrogen bond, in this case involving N3H···O1. The electronic density maps analysis also confirmed the presence of the hydrogen atoms bonded to the nitrogen atoms N2 and N3.

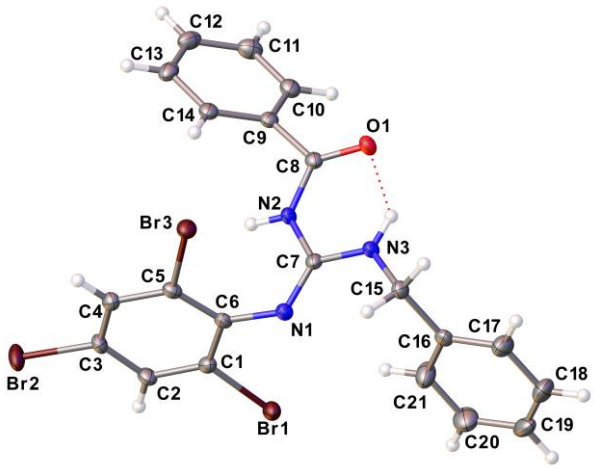

Preprints (www.preprints.org) | NOT PEER-REVIEWED | Posted: 22 December 2023 doi:10.20944/preprints202312.1728.v1



**Figure 3.** ORTEP type representation of the asymmetric unit of LQOF-G35-Br. Thermal ellipsoids are represented with 50% of probability.

To better understanding the conformational change, LQOF-G35 was subjected to 12 hours of infrared irradiation and subsequently analyzed by $^{1}$H NMR. This experiment revealed that without NBS the initial ***Z*** conformation of LQOF-G35 was maintained. Therefore, the polybromination was responsible for this conformational change in LQOF-G35-Br, more specifically the entry of the second atom of bromo, which was confirmed because the compound with two bromine atoms in the aniline ring was synthesized and it showed only the ***Z*** conformation.

The *Z*/*E* conformational ratio is directly related to the position of the double bond N10=C9 (Figure 1). The entry of the second atom of bromo in the aniline moiety, promote the increase in energy resulting in the opening of the *pi* bond and subsequent rotation around the N10-C9 sigma bond to reach the ***E*** conformation with the restored double bond localized between in N10=C9.

*3.1. Structural data of compounds*

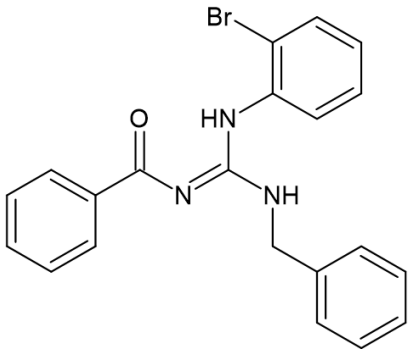


(*Z*)-*N*-benzoyl-*N*-benzyl-*N*-(2-bromophenyl)guanidine (LQOF-G35). MM: 407.06 g.mol$^{-1}$. White solid. Melting point: 103-104°C. $^{1}$H NMR 263K (500.16 MHz, $CDCl_3$) δ Z isomer = 12.33 (s, 1H), 8.30 (d, 2H), 7.69 (d, 1H), 7.50 (q, 2H), 7.43 (t, 3H), 7.41 – 7.34 (m, 4H), 7.31 (m, 1H), 7.16 (t, 1H), 5.19 (t, 1H), 4.84 (d, 2H). $^{13}$C NMR (125.765 MHz, $CDCl_3$) δ = 177.7 (C=O), 158.1 (C=N), 138.2 (C), 137.8 (C), 134.6 (C), 134.0 (CH), 131.4 (CH), 129.1 (CH), 128.8 (CH), 128.7 (CH), 127.9 (CH), 127.6 (CH), 127.5 (CH), 127.4 (CH), 121.2 (C-Br), 45.0 (N-$CH_2$). GC-MS/EI (m/z 406). ESI(+)-MS *m*/*z* found 408.0705, *m*/*z* calculated for $[C_{21}H_{18}BrN_3O + H]^+$: 408.0706; ESI(+)-MS/MS: $M + H - C_6H_5CONH_2]^+$ *m*/*z* 287.0175, $[M + H - C_{15}H_{12}N_2O]^+$ *m*/*z* 171.9757, $[M + H - C_{13}H_{12}BrN_2]^+$ *m*/*z* 122.0603;

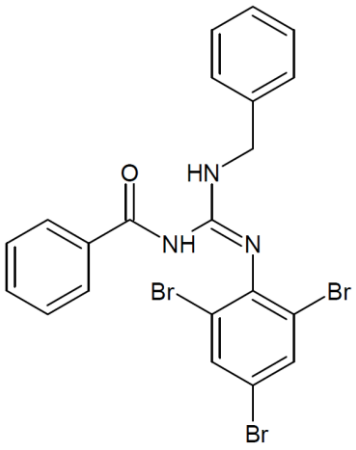


(*E*)-*N*-benzoyl-*N*-benzyl-*N*-(2,4,6-*tri*-bromophenyl)guanidine (LQOF-G35-Br). MM: 566.09 g.mol-1. White solid. Melting point: 148-149°C. $^{1}$H NMR 10 °C (500.16 MHz, $CDCl_3$) δ *E* isomer 8.86 (s, 1H), 8.22 (s, 1H), 7.73 (s, 2H), 7.62 – 7.53 (m, 3H), 7.51 – 7.43 (m, 6H), 7.37 (t, 3H), 7.32 – 7.27 (m, 2H), 4.72 (d, 2H). $^{13}$C NMR (125.765 MHz, $CDCl_3$) δ = 166.6 (C=O), 144.4 (C=N), 143.6 (C-Br), 138.1 (C), 134.6

Preprints (www.preprints.org) | NOT PEER-REVIEWED | Posted: 22 December 2023 doi:10.20944/preprints202312.1728.v1



(CH), 133.2 (CH), 132.8 (C), 129.2 (CH), 128.6 (CH), 127.7 (CH), 127.3 (CH), 127.0 (CH), 119.3 (C), 115.4 (2C-Br), 45.0 (N-CH2). GC-MS/EI (m/z 565): 77, 91, 105, 122, 285, 406, 486. HRESI-MS m/z 565.8898 [M+H]+ (calcd for C21H16Br3N3O1, 566.091, Δ= -0.2012 ppm). Ionic fragment observed in ESI(+)-MS/MS: [M+H–$C_{14}H_{11}BrN_2O$]+ m/z 486.5555.

## 4. Materials and Methods

### *4.1. Guanidine bromination using NBS and IR irradiation with a IR lamp (150 Watts)*

As a bromination method, N-Bromosuccinimide (NBS) catalyzed by 150-watt infrared light was used, under magnetic stirring for 12 hours (Scheme 1), a reflux system was added to avoid evaporating the solvent (Dichloromethane). This choice was motivated by the commercial availability of NBS and its good stability, which minimizes self-decomposition. Furthermore, NBS is compatible with the solubility of guanidines. The reaction was performed using a molar relationship guanidine: NBS of 1 mol of guanidine to 1.4 mol of NBS. After the reaction end, the reaction mixture was cooled to 10ºC and washed with water, then the organic layer (dichloromethane) was separated and dried on magnesium sulfate. Subsequently, the reaction mixture was filtered, the solvent was evaporated, and the cru product was recrystallized from a mixture of petroleum ether and diethyl ether (9:1 v/v). Then, the suspension was filtered off and the solid was dried by reduced pressure and suspended in ethanol with ultrasound and recrystallized one more time.

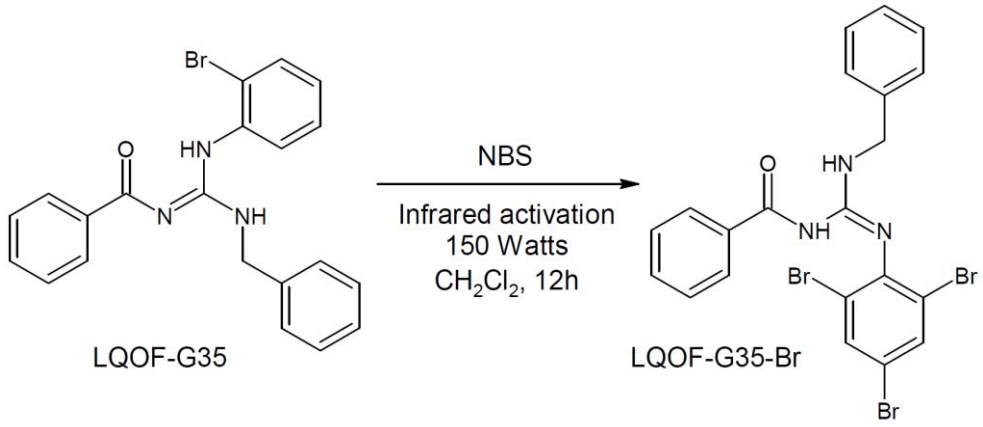


**Scheme 1.** Bromination of the compound LQOF-G35 with formation of the polybrominated compound LQOF-G35-Br as confirmed by XRD.

### *4.2. Melting point*

Melting point was obtained using a WRS-2 Micro Processor Melting-point apparatus. The samples were placed in a capillary tube, and pre-heating and final ramp temperatures were selected for 60°C and 250°C, respectively. The heating rate used was 2.0°C/min.

### *4.3. Electronic ionization mass spectrometry*

The mass spectra of the guanidines were acquired by direct introduction (DI) in the Mass Spectrometry, with a Shimadzu QP-2010 Plus equipment with Electron Ionization (EI). The parameters used for the analysis were: Interface temperature: 240°C; Ionization chamber: 300°C; Time to solvent cut; 0.5 min; Initial time: 0.7 min; Final time: 25 min; DI temperature program: Initial temperature: 50°C, with heating from 20°C/min to 350°C and standby time 10min. The analysis was performed using acetonitrile and dichloromethane as a solvent. The energy used for ionization was 70ev.

### *4.4. RMN*

$^{1}H$, $^{13}C$ and other 2D NMR spectra were recorded on a Bruker Avance III-HD – 500 MHz. The resonance frequency for $^{1}H$ NMR was 500.16 MHz and for $^{13}C$ NMR 125.765 MHz. Chemical shifts

 doi:10.20944/preprints202312.1728.v1



for $^{1}H$ NMR and $^{13}C$ NMR were referenced to TMS, analysis was performed in $CDCl_3$ and all chemical shifts were reported in ppm. Data are presented as following: chemical shift, multiplicity (s = singlet, d = doublet, dd = doublet of doublet, t = triplet, qua = quadruplet, qu = quintuplet, m = multiplet, br s = broad singlet), integration, and coupling constants (in Hertz).

*4.5. HRESIMS*

The UPLC-ESI-QTOF-MS/MS analysis was performed on a Waters modular UHPLC consisting of a QSM Acquity® HClass quaternary pump, an Acquity® Sample Manager – FTM autosampler, and an Acquity® PDAeλ diode array detector, hyphenated to a Waters Xevo® G2-XS mass spectrometer, equipped with an electrospray ionization source (ESI), a quadrupole analyzer, and a collision cell configured in sequence with a time-of-flight (TOF) analyzer. The chromatographic separation was performed in gradient mode using a solution of formic acid at 0.1% v/v as mobile phase in ultrapure water as component A and acetonitrile acidified with formic acid at a concentration of 0.1% v/v as component B. Chromatographic runs were performed at a flow rate of 0.5 mL.min-1, starting with 5% of component B in the mobile phase composition. The variation of the elution force was programmed so that in 5 min the %B increased until reaching the value of 100%. The analysis was performed on a Waters Acquity® UPLC HSS T3 reversed phase column (C18) containing 1.8 µm particles with 2.1 mm internal diameter and 100 mm length. The injection volume applied to the column was 0.2 µL. Full scan and MS/MS mass spectra were acquired in positive mode in the range of m/z 100 to 1500. Electrospray capillary and transfer cone voltages were maintained at (+) 2.5 kV and 20V respectively. The ESI source and desolvation gas temperatures were set to 120.0 and 350.0 °C respectively. The acquisition of MS/MS spectra was performed in Fast DDA mode (data dependent acquisition), in which only ions with intensity above 100 were fragmented. Ion fragmentation was performed by applying a voltage ramp so that for m/z 100 the energy ranged from 10 to 40 eV and for m/z 1500, from 40 to 70 eV.

*4.6. Single crystal X-ray diffraction (SCXRD)*

Single crystals of LQOF-G35 and LQOF-G35-Br were obtained and analyzed at 100 K on a Rigaku XtaLAB Synergy-S Dualflex diffractometer equipped with an HyPix 6000HE detector, using a Cu Kα radiation (1.54184 Å). Data collection, cell refinement, data reduction and absorption correction were performed using the CrysAlisPro software [31]. Intrinsic phasing method from the SHELXT-2018/2 program [32] was used to solve the structures, while the refinement of the non-hydrogen atoms was performed with non-linear the least-squares minimization on $F^2$ using the SHELXL-2019/2 program [33] and considering anisotropic displacement parameters. Hydrogen atoms were calculated at idealized positions using the riding model. The calculated positions of the hydrogen atoms bonded to the nitrogen atoms from the guanidine group were confirmed by the analyses of the electron density maps. Olex2 [34] was used for the solution and refinement of the structures, and to generate the graphical illustrations. Tables containing the information about the data collection, refinement and structural parameters are available in the Supplementary Materials.

The CIF file of LQOF-G35 and LQOF-G35-Br were deposited in the Cambridge Structural Data Base with CCDC number 2320314 and 23200315, respectively. Copies of the data can be obtained, free of charge, via www.ccdc.cam.ac.uk.

**5. Conclusions**

Two guanidine compounds have been unambiguously characterized. MS-EI and HRESI-MS analyzes showed one bromine atom in the compound LQOF-G35 and three Br in LQOF-G35-Br structures.

NMR and DRX have confirmed that all the bromine atoms are in the aniline ring. A conformational change from Z to E had also corroborated by these studies.

Finally, existence of the guanidine compound containing two-Br atoms on the same aniline ring, is strong evidence of the conformational change is occurring simultaneously to second bromine entrance.

**Supplementary Materials:** The following supporting information can be downloaded at: www.mdpi.com/xxx/s1, Figure S1: EI-MS (70 eV) spectrum of compound LQOF-G35 is displayed below; Figure S2: EI-MS (70 eV) spectrum of compound LQOF-G35-Br is displayed below; Figure S3: HRESI-MS Spectrum of LQOF-G35-Br; Figure S4. HPLC-UV analysis of LQOF-G35; Figure. S5. HRESI-(+) MS analysis of LQOF-G35; Figure. S6. HRESI-(+) MS/MS analysis of LQOF-G35.Figure S7: $^{1}H$ NMR spectrum of the aromatic region for LQOF-G35 at 263K in $CDCl_3$, Figure S8: $^{13}C$ NMR spectrum for LQOF-G35 at 263K in $CDCl_3$; Figure S9: HMBC $^{1}Hx^{15}N$ NMR spectrum for LQOF-G35 at 263K in $CDCl_3$; Figure S10: HSQC $^{1}Hx^{13}C$ NMR spectrum for LQOF-G35 at 263K in $CDCl_3$; Figure S11: HMBC $^{1}Hx^{13}C$ NMR spectrum for LQOF-G35 at 263K in $CDCl_3$; Figure S12: NOESY $^{1}Hx^{1}H$ NMR spectrum for LQOF-G35 at 263K in $CDCl_3$; Figure S13: $^{1}H$ NMR spectrum for LQOF-G35-Br at 283K in $CDCl_3$; Figure S14: $^{13}C$ DEPTQ-135 NMR spectrum for LQOF-G35-Br at 283K in $CDCl_3$; Figure S15: HMBC $^{1}Hx^{13}C$ NMR spectrum for LQOF-G35-Br at 283K in $CDCl_3$; Figure S16: HSQC $^{1}Hx^{13}C$ NMR spectrum for LQOF-G35-Br at 283K in $CDCl_3$; Figure S17: NOESY $^{1}Hx^{1}H$ NMR spectrum for LQOF-G35-Br at 283K in $CDCl_3$; Table S1: Crystal data and refinement parameters of LQOF-G35 and LQOF-G35-Br.; Table S2: Selected bond lengths and angles for LQOF-G35; Table S3: Selected bond lengths and angles for LQOF-G35-Br.

**Author Contributions:** E.H.Z.—organic synthesis and, NMR and DRX conformational study; L.R.d.A.— organic synthesis and NMR conformational study; P.H.d.O.S. — X-ray measurements and process for conformational study; T.R.d.S.N. — organic synthesis; J.A.E — X-ray measurements, process for conformational study and supervision; E.R.P.G.—general supervision. All authors have read and agreed to the published version of the manuscript.

**Funding:** This research received no external funding.

**Data Availability Statement:** No applicable.

**Acknowledgments:** Luana Ribeiro dos Anjos thanks to CAPES for postgraduation fellowships. Eduardo R. P. Gonzalez thanks to FAPESP for financial support (funding 2021/0595-8) and to UNESP–MCTI-IEAMAR and FAPESP (2018/00581-7 and 2021/2595-8) for 500 MHz Bruker Nmr apparatus. Eduardo R. Perez Gonzalez is thankful to Agreement FINEP 01.23.0034.00 (0419/22) – "Study and identification of active compounds against cutaneous and visceral leishmaniasis: from discovery to preclinical study", Process FUNDUNESP - CCP nº 3348/2022. Pedro H. O. Santiago thanks to FAPESP (2021/10066-5). Javier Ellena is grateful to FAPESP (2017/15850-0) and CNPq (312505/2021-3).

**Conflicts of Interest:** The authors declare no conflict of interest.

## References

1. World Health Organization, Leishmaniasis. Available online: https://www.who.int/news-room/fact-sheets/detail/leishmaniasis (accessed on 02 December 2023).
2. I. Abadías-Granado, A. Diago, P.A. Cerro, A.M. Palma-Ruiz, Y. Gilaberte. Cutaneous and Mucocutaneous Leishmaniasis. Actas Dermo-Sifiliográficas (English Edition), 2021, Volume 112, Issue 7, Pages 601-618.
3. Cecílio, P., Cordeiro-da-Silva, A. & Oliveira, F. Sand flies: Basic information on the vectors of leishmaniasis and their interactions with Leishmania parasites. Commun Biol, 2022, Volume 5, Page 305.
4. Ikeogu, N.M.; Akaluka, G.N.; Edechi, C.A.; Salako, E.S.; Onyilagha, C.; Barazandeh, A.F.; Uzonna, J.E. Leishmania Immunity: Advancing Immunotherapy and Vaccine Development. Microorganisms 2020, Volume 8, Page 1201.
5. S. Pradhan, R.A. Schwartz, A. Patil, S. Grabbe, M. Goldust, Treatment options for leishmaniasis, Clinical and Experimental Dermatology, 2022, Volume 47, Issue 3, Pages 516–521.
6. Basmaciyan L, Casanova M. Cell death in Leishmania. Parasite, 2019, Vol 26, Page 71.
7. Spasov, A.; Ozerov, A.; Kosolapov, V.; Gurova, N.; Kucheryavenko, A.; Naumenko, L.; Babkov, D.; Sirotenko, V.; Taran, A.; Borisov, A.; et al. Guanidine Derivatives of Quinazoline-2,4(1H,3H)-Dione as NHE-1 Inhibitors and Anti-Inflammatory Agents. Life 2022, 12, 1647.
8. Christie Morrill, Westley J. Friesen, Suresh Babu, Ramil Y. Baiazitov, Wu Du, Diane B. Karloff, Chang-Sun Lee, Young-Choon Moon, Hongyu Ren, Jairo Sierra, Yuki Tomizawa, Priya Vazirani, Ellen M. Welch, Xiaojiao Xue, Jin Zhuo. Guanidino quinazolines and pyrimidines promote readthrough of premature termination codons in cells with native nonsense mutations, Bioorganic & Medicinal Chemistry Letters, Volume 76, 2022, 128989.
9. Yoshiaki Yoshida, Takeshi Endo. Synthesis of multifunctional 4-hydroxymethyl 2-oxazolidinones from glycidyl carbamate derivatives catalyzed by bicyclic guanidine, Tetrahedron Letters, Volume 72, 2021, 153086.

10. Rama M. Shakaroun, Philippe Jéhan, Ali Alaaeddine, Jean-François Carpentier and Sophie M. Guillaume, Organocatalyzed ring-opening polymerization (ROP) of functional β-lactones: new insights into the ROP mechanism and poly(hydroxyalkanoate)s (PHAs) macromolecular structure. Polym. Chem., 2020,11, 2640-2652.
11. Ángela Mesías-Salazar, Javier Martínez, René S. Rojas, Fernando Carrillo-Hermosilla, Alberto Ramos, Rafael Fernández-Galánb and Antonio Antiñolo. Aromatic guanidines as highly active binary catalytic systems for the fixation of CO2 into cyclic carbonates under mild conditions. Catal. Sci. Technol., 2019,9, 3879-3886.
12. Korolkova, Y.; Makarieva, T.; Tabakmakher, K.; Shubina, L.; Kudryashova, E.; Andreev, Y.; Mosharova, I.; Lee, H.-S.; Lee, Y.-J.; Kozlov, S. Marine Cyclic Guanidine Alkaloids Monanchomycalin B and Urupocidin A Act as Inhibitors of TRPV1, TRPV2 and TRPV3, but not TRPA1 Receptors. Mar. Drugs 2017, 15, 87.
13. Staszewski, M.; Iwan, M.; Werner, T.; Bajda, M.; Godyń, J.; Latacz, G.; Korga-Plewko, A.; Kubik, J.; Szałaj, N.; Stark, H.; et al. Guanidines: Synthesis of Novel Histamine H3R Antagonists with Additional Breast Anticancer Activity and Cholinesterases Inhibitory Effect. Pharmaceuticals 2023, 16, 675.
14. Madiha A. Siddiqui, Amol A. Nagargoje, Mubarak H. Shaikh, Rashiqua A. Siddiqui, Amit A. Pund, Vijay M. Khedkar, Ashish Asrondkar, Prathmesh P. Deshpande & Bapurao B. Shingate. Design, Synthesis and Bioevaluation of Highly Functionalized 1,2,3-Triazole-Guanidine Conjugates as Anti-Inflammatory and Antioxidant Agents, Polycyclic Aromatic Compounds, 2023, 43:6, 5567-5581,
15. Shumaila Zubair, Amin Badshah, Jahangeer Patujo, Mehmand Khan, Ahmad Raheel, Faiza Asghar, Shamila Imtiaz. New ferrocene integrated amphiphilic guanidines: Synthesis, spectroscopic elucidation, DFT calculation and in vitro $\alpha$-amylase and $\alpha$-glucosidase inhibition combined with molecular docking approach. Heliyon, 2023, 9 e14919.
16. Cao, Y., Gu, J., Wang, S. et al. Guanidine-functionalized cotton fabrics for achieving permanent antibacterial activity without compromising their physicochemical properties and cytocompatibility. Cellulose 27, 6027–6036 (2020).
17. Xiufeng Zhang, Dongdong Han, Pengfei Pei, Jie Hao, Yixing Lu, Peng Wan, Xianfeng Peng, Weibiao Lv, Wenguang Xiong & Zhenling Zeng, In vitro Antibacterial Activity of Isopropoxy Benzene Guanidine Against Multidrug-Resistant Enterococci, Infection and Drug Resistance, 2019, 12:, 3943-3953.
18. Baugh, S.D.P. Guanidine-Containing Antifungal Agents against Human-Relevant Fungal Pathogens (2004–2022)—A Review. J. Fungi 2022, 8, 1085.
19. Ana R. Gomes, Carla L. Varela, Ana S. Pires, Elisiário J. Tavares-da-Silva, Fernanda M.F. Roleira, Synthetic and natural guanidine derivatives as antitumor and antimicrobial agents: A review, Bioorganic Chemistry, 2023, Volume 138, 106600.
20. R.D. do Espírito Santo et al. N, N`, N``-trisubstituted guanidines: Synthesis, characterization and evaluation of their leishmanicidal activity. European Journal of Medicinal Chemistry, 2019, 171, 116e128.
21. Natalia C. S. Costa, Luana Ribeiro dos Anjos, João Victor Marcelino de Souza, Maria Carolina Oliveira de Arruda Brasil, Vitor Partite Moreira, Marcia A. S. Graminha, Gert Lubec, Eduardo Rene P. Gonzalez*, and Eduardo Maffud Cilli. Development of New Leishmanicidal Compounds via Bioconjugation of Antimicrobial Peptides and Antileishmanial Guanidines, ACS Omega 2023, 8, 37, 34008–34016.
22. Moreira, V.P.; da Silva Mela, M.F.; Anjos, L.R.d.; Saraiva, L.F.; Arenas Velásquez, A.M.; Kalaba, P.; Fabisiková, A.; Clementino, L.d.C.; Aufy, M.; Studenik, C.; et al. Novel Selective and Low-Toxic Inhibitor of LmCPB2.8ΔCTE (CPB) One Important Cysteine Protease for Leishmania Virulence. Biomolecules 2022, 12, 1903. https://doi.org/10.3390/biom12121903
23. Almeida, F.S.; Moreira, V.P.; Silva, E.d.S.; Cardoso, L.L.; de Sousa Palmeira, P.H.; Cavalcante-Silva, L.H.A.; Araújo, D.A.M.d.; Amaral, I.P.G.d.; González, E.R.P.; Keesen, T.S.L. Leishmanicidal Activity of Guanidine Derivatives against Leishmania infantum. Trop. Med. Infect. Dis. 2023, 8, 141.
24. ANJOS, L. R.; DE SOUZA, V. M. R.; MACHADO, Y. A. A.; PARTITE, V. M.; AUFY, M.; DIAS-LOPES, G.; STUDENIK, C.; ALVES, C. R.; LUBEC, G.; GONZÁLEZ, E. R. P.; RODRIGUES, K. A. F. Evidence of guanidines potential against Leishmania (Viannia) braziliensis: Exploring in vitro effectiveness, toxicities and of innate immunity response effects. Fine Organic Chemistry Lab, School of Sciences and Technology, São Paulo State University (UNESP), Presidente Prudente, São Paulo, Brazil. Brazil Infectious Disease Laboratory– LADIC, Federal university of Parnaíba Delta - UFDPar, Campus Ministro Reis Velloso, São Benedito, Parnaíba-PI, Brazil. 2023, manuscript submitted.
25. Isac-García, J., Dobado, J. A., Calvo-Flores, F. G., & Martínez-García, H., Microscale Experiments. Experimental Organic Chemistry: Laboratory Manual. 2016, 371-408.
26. Ji Ram, V., Sethi, A., Nath, M., & Pratap, R. Five-Membered Heterocycles. The Chemistry of Heterocycles, 2019, 149–478.
27. Barnes, R. A. N-Bromosuccinimide as a Dehydrogenating Agent1. Journal of the American Chemical Society, 1948, 70(1), 145–147.
28. Sivakamasundari, S., & Ganesan, R. Kinetics and mechanism of the bromination of aromatic compounds byN-bromosuccinimide in solution. International Journal of Chemical Kinetics, 1980, 12(11), 837–850.

 doi:10.20944/preprints202312.1728.v1




29. Appa, R.M., Naidu, B.R., Lakshmidevi, J. et al. Added catalyst-free, versatile and environment beneficial bromination of (hetero)aromatics using NBS in WEPA. SN Appl. Sci. 2019, 1, 1281.
30. Sanghyuck Lee, and Choon Sup Ra. Benzylic Brominations with N-Bromosuccinimide in 1,2-Dichlorobenzene: Effective Preparation of (2-Bromomethyl-phenyl)-Methoxyiminoacetic Acid Methyl Ester. Clean Technol., 2016, Vol. 22, No. 4, pp. 269-273.
31. Oxford Diffraction /Agilent Technologies UK Ltd CrysAlisPRO
32. Sheldrick, G.M. SHELXT – Integrated space-group and crystalstructure determination. Acta Cryst. (2015). A71, 3–8.
33. Sheldrick, G.M. Crystal structure refinement with SHELXL. Acta Cryst. (2015). C71, 3–8.
34. O.V. Dolomanov and L.J. Bourhis and R.J. Gildea and J.A.K. Howard and H. Puschmann, Olex2: A complete structure solution, refinement and analysis program, J. Appl. Cryst., (2009), 42, 339-341.